



Temperature dependency of MOSFET device characteristics in 4H- and 6H-silicon carbide (SiC)

Md Hasanuzzaman^{a,*}, Syed K. Islam^{a,b}, Leon M. Tolbert^{a,b},
 Mohammad T. Alam^a

^a Department of Electrical and Computer Engineering, The University of Tennessee, Knoxville, TN 37996-2100, USA

^b Oak Ridge National Laboratory, National Transportation Research Center, Oak Ridge, TN 37831-6472, USA

The review of this paper was arranged by Prof. A. Iliadis

Abstract

The advantages of silicon carbide (SiC) over silicon are significant for high power and high temperature device applications. An analytical model for a lateral MOSFET that includes the effects of temperature variation in 6H-SiC poly-type has been developed. The model has also been used to study the device behavior in 4H-SiC at high ambient temperature. The model includes the effects of temperature on the threshold voltage, the carrier mobility, the body leakage current, and the drain and source contact region resistances. The MOSFET output characteristics and parameter values have been compared with previously measured experimental data. A good agreement between the analytical model and the experimental data has been observed. 6H-SiC material system provides enhanced device performance compared to 4H-SiC counterpart for lateral MOSFET.

© 2004 Elsevier Ltd. All rights reserved.

Keywords: High temperature MOSFET; Silicon carbide; Temperature variation effect

1. Introduction

Silicon carbide, a wide bandgap material, shows a tremendous potential for high temperature electronics applications and offers significant advantages for power switching devices. It has a high electric breakdown field (3.5×10^6 V/cm), high electron saturated drift velocity (2×10^7 cm/s), high melting point (2830 °C), and high thermal conductivity (4.9 W/cm K) that give it a great potential for high temperature and high power device applications. SiC is the most advanced wide bandgap material in the context of better quality material growth, defect free dielectric formation, implantation doping, contacts via metallization, and other process steps. Recent progresses in SiC make it likely that a manufac-

turable MOSFET device technology can be developed within the next three to five years [1–4].

MOSFETs are widely used in amplifier design, analog integrated circuits, digital CMOS design, power electronics and switching devices. A model for a vertical MOSFET, which is a suitable structure for a power MOSFET, has been developed, and its impact on the system level benefits of SiC MOSFET has been studied and reported [5–7]. A systematic investigation of silicon devices for high temperature electronics (MOSFETs, as well as CMOS technology) was reported by Shoucair et al. [8,9]. Temperature dependency of the model parameters of 6H-SiC MOSFET was explained from the measured data [10]. A CMOS process has been developed, fabricated and tested in 6H-SiC [11]. The measured data for NMOS and PMOS output and transfer characteristics, threshold voltage, and sheet resistances was reported in [11]. This paper presents an analytical model for a lateral MOSFET in 6H-SiC that includes the effects of temperature on the threshold voltage,

* Corresponding author. Tel.: +1-865-974-9882; fax: +1-865-974-5483.

E-mail address: mhasanuz@utk.edu (M. Hasanuzzaman).

carrier mobility, the body leakage current, and the drain and source contact region resistances. Preliminary results from the analytical model and the measured data presented in [11] demonstrate the feasibility of the developed model.

2. Proposed model

A large-signal model for a lateral MOSFET with temperature compensation has been proposed (Fig. 1). The temperature dependent compensating current elements are considered to be in parallel with the MOSFET channel between the drain and the source. These currents contribute to the total current at high temperature. The three compensating current elements are: (i) the body leakage current, I_R ; (ii) the current change due to the threshold voltage change, I_{TH} ; and (iii) the current change due to the change of drain and source contact region resistance, I_{RDS} . The calculations are performed using room temperature (300 K) as the reference temperature. MOSFET channel current, I_D , has been calculated using Eqs. (1) and (2) which are obtained from a MOSFET charge sheet model [12]. Channel current, I_D , is kept constant for all temperature. The compensating currents incorporate the change in the MOSFETs current.

$$I_D = \frac{W}{L} \mu_n C_{ox} [(V_{GS} - V_{TH}) - V_{DS}/2] V_{DS} \quad (1)$$

$$I_{D_{sat}} = \frac{W}{2L} \mu_n C_{ox} (V_{GS} - V_{TH})^2 \quad (2)$$

where, the symbols have their usual meaning. Eq. (1) is used in the linear region of operation and Eq. (2) is used in the saturation region of operation of the MOSFET.

The total drain current can be expressed as Eq. (3);

$$I_{total} = I_D + I_R + I_{TH} + I_{RDS} \quad (3)$$

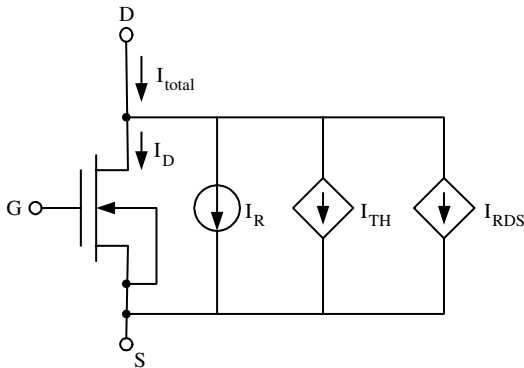


Fig. 1. MOSFET model with temperature compensation.

where

$$I_R = qA \frac{D_n n_i^2}{L_n N_A} \alpha A T^3 \exp \left\{ -\frac{E_g}{kT} \right\} \quad (4)$$

$$I_{TH} = \frac{W}{L} \mu_n C_{ox} [V'_{TH} - V_{TH}] V_{DS} \quad (5)$$

$$I_{TH_{sat}} = \frac{W}{2L} \mu_n C_{ox} [(V_{GS} - V'_{TH})^2 - (V_{GS} - V_{TH})^2] \quad (6)$$

$$I_{RDS} = \beta \left(\frac{1}{R'_{DS}} - \frac{1}{R_{DS}} \right) V_{DS} \quad (7)$$

The change in current due to leakage current is given by Eq. (4). The change in current due to the change in threshold voltage is evaluated by Eq. (5) for linear region of operation and by Eq. (6) for saturation region of operation. At room temperature, I_R is negligible, and I_{TH} and I_{RDS} become zero. However, with the increase in temperature, compensating terms contribute to the total current.

2.1. Leakage currents

The contribution of the leakage current at room temperature is negligible. However, with the increase in temperature, intrinsic carrier concentration (n_i) increases exponentially. Therefore, the leakage current contributes to the total currents at high temperature. For an n-channel MOSFET device, the temperature dependence of the leakage current can be expressed by Eq. (4), which is basically the reverse saturation current of a diode. The existence of the leakage current can be shown in the large-signal MOSFET model by placing a diode between the drain and the body terminal, which is equivalent to a temperature dependent current source between the drain and the source terminals.

2.2. Threshold voltage

Threshold voltage is the most significant parameter in the study of temperature dependence of MOSFET characteristics. MOSFET current–voltage characteristics are proportional to the square of the difference of gate voltage and threshold voltage. Thus, a small change in threshold voltage causes a large change in the output current. Therefore, it is very important to calculate the threshold voltage accurately with temperature changes. There are many material parameters that are related to the calculation of threshold voltage, and a number of empirical relationships have been obtained from the experimental data [13].

2.3. Mobility

Surface roughness and high interface state density play important roles in inversion layer mobility. Experimentally measured mobility values in the inversion layer have been reported in [10,11]. The reported values show an interesting trend in the mobility. Initially, the carrier mobility increases with temperature (contrary to the normal behavior of mobility) for a working temperature range of 300–500 K. This may be due to the early movement of Fermi level towards the band gap with increased temperature. However, the mobility decreases at very high temperature where lattice scattering dominates and begins to release the interface trap charges. Therefore, the inversion layer mobility is almost constant over the temperature range (300–600 K) considered in the model.

2.4. Contact region resistances

The drain and the source metal contact resistances and n+ region sheet resistance of the MOSFET also change with temperature. It is shown in [11] that the value of sheet resistance of the 6H-SiC lateral MOSFET at 600 K becomes almost half of the value at 300 K. The resistance values decrease almost linearly. Therefore, a linear approximation has been made in the calculation of the resistances. The resistance of the metallic contact is negligible due to larger contact area. Therefore, only the change of the sheet resistance has been considered into the resistance calculation. The change in the drain and the source resistances has been modeled as a change in conductance.

3. Results and discussion

The model has been evaluated in 6H-SiC material system, and the same device dimensions as those of [11] are used for simulations. The measured data were reported in [11] for a lateral MOSFET fabricated in 6H-SiC. The output characteristics have been simulated at 300, 400, 500 and 600 K. Figs. 2 and 3 show the output characteristics for simulated and measured data at 300 and 600 K, respectively. The simulation results match perfectly with the measured data at 300 K as compared to the results at 600 K where there are minor discrepancies. At 300 K, the drain current is 15 μA , whereas it rises to 235 μA at 600 K for a gate voltage $V_{GS} = 6\text{ V}$.

The changes in threshold voltage with temperature are also simulated and compared with measured data as shown in Fig. 4. The SiC lateral MOSFET has a very high threshold voltage, ($\approx 3.2\text{ V}$) at room temperature and 1.2 V at 600 K [11]. The large variation of the threshold voltage causes a huge change in the drain currents of the MOSFET.

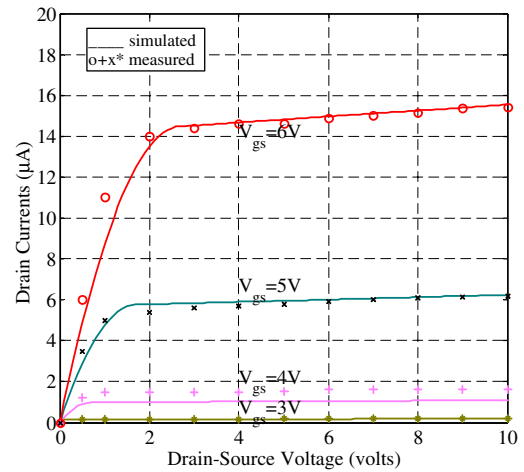


Fig. 2. Output characteristics at 300 K.

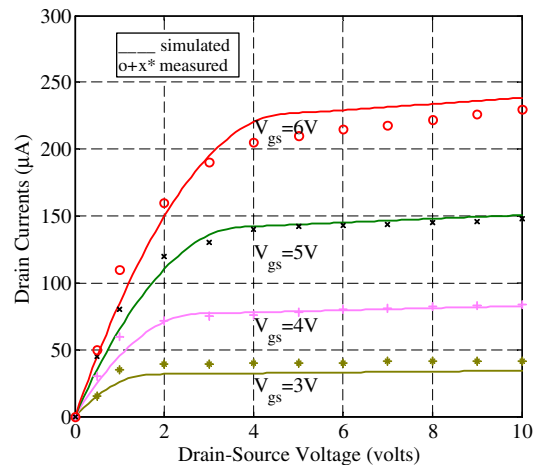


Fig. 3. Output characteristics at 600 K.

The simulation results demonstrate a very good agreement with the measured threshold voltage values. The contributions of the compensating currents to the total current change are evaluated at different temperatures. Table 1 shows the relative contribution of the compensating currents to the total currents. It has been observed that most of the current change (about 85% on an average) is due to the threshold voltage change. Thus, the threshold voltage mostly characterizes the device behavior. At lower temperature, contribution of the leakage current is negligible. However, at high temperature it plays a major role. Drain and source resistances change monotonously with temperature.

The model is also used to simulate the device characteristics in 4H-SiC material system. Since the model showed a good agreement with measured data for 6H-SiC, simulation results for 4H-SiC is also reasonable and

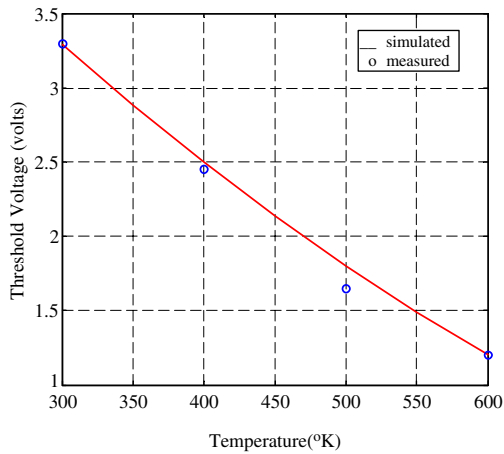


Fig. 4. Threshold voltages obtained from simulation and measurement for different temperature.

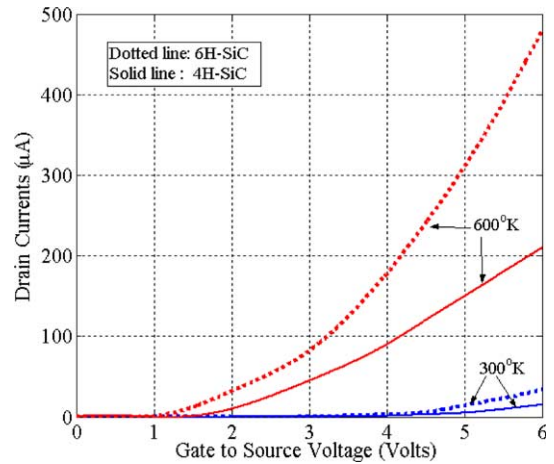


Fig. 6. Transfer characteristics of 4H- and 6H-SiC lateral MOSFET.

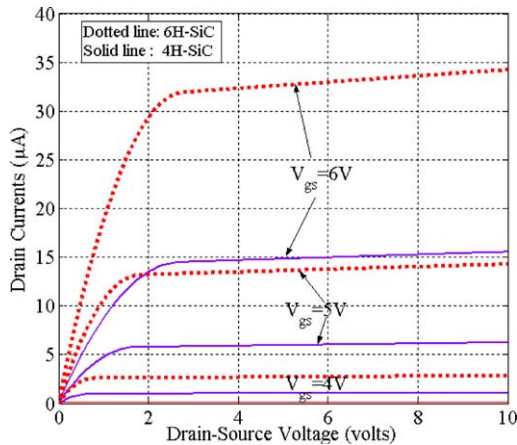


Fig. 5. Output characteristics of 4H- and 6H-SiC lateral MOSFET.

acceptable for prediction of device behavior in 4H-SiC. Figs. 5 and 6 show the comparison of the output characteristics of 4H- and 6H-SiC MOSFET at 300 K and transfer characteristics at different temperature, respectively. Simulation results show that the drain currents of 6H-SiC MOSFET are greater than that of 4H-SiC counterpart by a factor of approximately two and half. This could be attributed to higher mobility values of 6H-

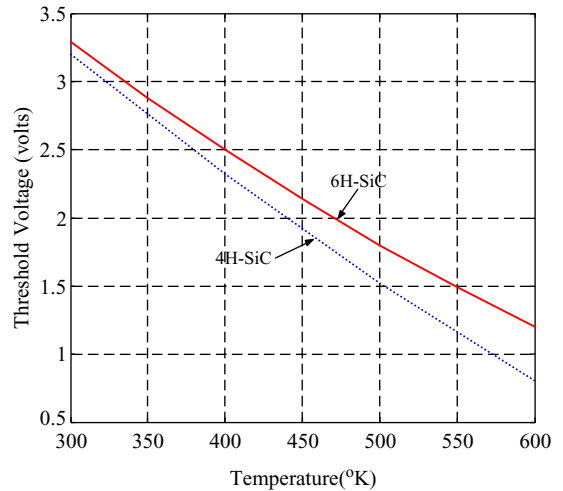


Fig. 7. Threshold voltage variation of 4H- and 6H-SiC lateral MOSFET with temperature.

SiC inversion layer ($\cong 100 \text{ cm}^2/\text{V s}$) compared to that of 4H-SiC ($\cong 40 \text{ cm}^2/\text{V s}$). The variation in the threshold voltage in 4H-SiC is also observed (Fig. 7). In summary, 6H-SiC material system provides enhanced device performance compared to 4H-SiC counterpart for lateral MOSFET.

Table 1
Contribution of the compensating currents to the total current change

| Temperature (K) | Total current change (μA) | Percentage of current change due to threshold voltage | Percentage of current change due to body leakage | Percentage of current change due to resistance |
|-----------------|--|---|--|--|
| 400 | 45 | 90 | 2 | 8 |
| 500 | 116 | 85 | 6 | 9 |
| 600 | 220 | 78 | 15 | 7 |

4. Conclusions

An analytical model has been developed to explain the behavior of the MOSFET output characteristics at different temperatures. The model has been evaluated for both 6H- and 4H-SiC material systems. The MOSFET output characteristics and parameter values are compared with previously measured experimental data. There is a good agreement between the model outputs and the experimental data. 6H-SiC material system provides enhanced device performance compared to 4H-SiC counterpart for lateral MOSFET.

Appendix A

List of abbreviation used in equations

| | |
|------------|---|
| I_D | drain current in linear region operation |
| I_{Dsat} | drain current in saturation region operation |
| I_R | body leakage current |
| I_{TH} | current due to threshold voltage change |
| I_{RDS} | current due to drain and source contact resistance |
| V_{GS} | gate to source voltage |
| V_{DS} | drain to source voltage |
| V_{TH} | threshold voltage at room temperature |
| V'_{TH} | threshold voltage at elevated temperature |
| R_{DS} | drain and source contact resistance at room temperature |
| R'_{DS} | drain and source contact resistance at elevated temperature |
| W | MOSFET channel width |
| L | MOSFET channel length |
| A | cross-sectional area |
| q | electron charge |
| μ_n | electron mobility |
| C_{ox} | oxide capacitance |
| α | proportionality constant |
| β | multiplying factor |

References

- [1] Powell A, Rowland L. SiC materials-progress, status, and potential roadblocks. *Proc IEEE* 2002;90(6):942–55.
- [2] Elasser A, Chow TP. Silicon carbide benefits and advantages for power electronics circuits and systems. *Proc IEEE* 2002;90(6):969–86.
- [3] Shenoy JN, Cooper JA, Melloch MR. High-voltage double implanted power MOSFETs in 6H-SiC. *IEEE Electron Dev Lett* 1997;18(3):93–5.
- [4] Agarwal AK, Casady JB, Rowland LB, Valek WF, White MH, Brandt CB. 1.1 kV 4H-SiC power UMOSFETs. *IEEE Electron Dev Lett* 1997;18(12):586–8.
- [5] Hasanuzzaman M, Islam SK, Tolbert LM. Effect of temperature variation (300–600 K) in MOSFET modeling in 6H silicon carbide. *Solid State Electron* 2004;48(1):125–32.
- [6] Hasanuzzaman M, Islam SK, Tolbert LM, Ozpineci B. Model simulation and verification of a vertical double implanted (DIMOS) transistor in 4H-SiC. In: *Proc the IASTED International Conference on Power System Palm Spring* 2003 p. 313–6.
- [7] Ozpineci B, Tolbert LM, Islam SK, Hasanuzzaman M. System impact of SiC power devices. *Int J High Speed Electron Syst* 2002;12(2):439–48.
- [8] Shoucair FS, Early JM. High temperature diffusion leakage current-dependent MOSFET small-signal conductance. *IEEE Trans Electron Dev* 1984;31(12):1866–72.
- [9] Shoucair FS. Design considerations in high temperature analog CMOS integrated circuits. *IEEE Trans Components, Hybrid Manufact Tech, CHMT* 1986;9(3):242–51.
- [10] Rebello NS, Shoucair FS, Palmour JW. 6H-Silicon carbide MOSFET modeling for high temperature analogue integrated circuits (25–500 °C). *IEE Proc—Circuits Dev Syst* 1996;143(2):115–22.
- [11] Ryu S-H. Development of CMOS technology for smart power applications in silicon carbide, PhD Thesis, Purdue University, May, 1997.
- [12] Casey HC. *Devices for integrated circuits, silicon and III–V compound semiconductors*. New York: John Wiley and Sons, Inc.; 1999.
- [13] Levinshtein ME, Rumyantsev SL, Shur MS. *Properties of advanced semiconductor materials*. The UK: John Wiley and Sons, Inc.; 2001.